Redistribution process of precipitation in ecological restoration activity of Pinus sylvestris var. mongolica in Mu Us Sandy Land, China

Yiben Cheng[1,2,3*], Hongbin Zhan[4], Wenbin Yang[5], Yunqi Wang[1,3], Qunou Jiang[1], Bin Wang[1,3]

[1]School of soil and water conservation, Beijing Forestry University, Beijing, China, 100083

[2]Yanchi Research Station, School of Soil and Water Conservation, Beijing Forestry University, Beijing 100083, China

[3]Jinyun Forest Ecosystem Research Station, School of Soil and Water Conservation, Beijing Forestry University, Beijing 100083, China

[4]Department of Geology and Geophysics, Texas A&M University, College Station, Texas, USA, 77843

[5] Inner Mongolia Low Coverage Company, Hohhot, 010000, China

Corresponding Author:

Yiben Cheng (chengyiben@bjfu.edu.cn)

Abstract: Precipitation was the most important water resource in semi-arid regions of China. The redistribution of precipitation among atmospheric water, soil water and groundwater are related to the land surface ecological system sustainability. The study took widely replanted Pinus sylvestris var. mongolica (PSM) in Mu Us Sandy Land (MUSL) as a research object and monitored precipitation, soil moisture, sap flow, and deep soil recharge (DSR) to find out moisture distribution in shallow soil layer. Results showed that the restoration process of PSM in MUSL changed the distribution of precipitation. Precipitation was intercepted in shallow soil, evapotranspiration increased, and DSR significantly decreased, resulting in up to 466.94 mm of precipitation returning to the atmosphere through evapotranspiration in 2016. Vegetation increased soil water storage (SWS) capacity, with maximum SWS in PSM plot and bare sandy land (BSL) being 260 mm and 197 mm per unit horizontal area, respectively in 2016. DSR decreased from 54.03% of precipitation in BSL to 0.2% of precipitation in PSM in 2016. Infiltration was not only intercepted by PSM ecosystem, resulting in a time lag, but was also affected by soil temperature, and the infiltration rate in the BSL plot was 11 times of that in the PSM plot from August to September in an annual base. SWS decreased 16 mm and 7.58 mm per unit horizontal area over a one-year period (from March to October) in 2017 and 2019, respectively. The PSM annual sap flow was maintained at a relatively constant level of 153.98 mm/yr. This study helps understand the role of precipitation-induced groundwater recharge in the process of vegetation restoration in semi-arid regions and explains the possible causes of PSM forest degradation. It is necessary to reduce PSM density to allow adaptation to extreme drought in the future.

Keywords: Three North Shelterbelt Project, Mu Us Sandy Land, Pinus sylvestris var Mongolica, Precipitation Redistribution, Deep Soil Recharge

1 Introduction

China's semi-arid regions have experienced serious and continuous ecological and environment

25   challenges for many decades with one third of the country was classified as desertification area

(Cao et al., 2011;Cao et al., 2018). To remedy the ecological and environmental problems in the

northern region of China, the Chinese government has implemented a large-scale vegetation

restoration plan. Since 1978, the Three-North Shelter Project (3NSP) has carried out a large-scale

vegetation restoration campaign in the arid and semi-arid regions of northern China (Zhang et al.,

30   2017;Deng et al., 2019). The goal of 3NSP is to increase the forest coverage in the Three-North

region from 5 % to 15 % by 2050. There are four ecological projects of vegetation restoration to

control desertification in the world (Shi et al., 2020;Wu et al., 2020), all of them choose to rebuild

vegetation in arid and semi-arid regions. Views on the results of afforestation are different. Some

researchers argue that the effect is significant, but others argue that afforestation has not reached

35   the expected ecological restoration goal for a variety of reasons (Lu et al., 2018;Han et al., 2020).

In view of the long-term influences of vegetation restoration in resolving environmental issues, we

need to evaluate vegetation restoration activities.

There are several evaluation methods for the advantages and disadvantages of vegetation

restoration, considering that water resources as the most important ecological factors in arid and

40   semi-arid regions (Yu et al., 2019;Azareh et al., 2019). Some researches have conducted a detailed

and systematic assessment of the hydrological process after vegetation restoration to understand

the impact of vegetation restoration on the local eco-hydrological environment (Bai et al.,

2020;Shao et al., 2019). 3NSP has alleviated some environmental problems in the north region of

China such as controlling the sandstorm and reducing the sandy soil erosion (An et al., 2019;Li et

45   al., 2017), but the impact of large-scale afforestation on the hydrological cycle is still largely

unknown (Krause et al., 2018;Doelman et al., 2020;Zeng et al., 2020). Large-scale afforestation can affect water cycle like consuming vast majority soil water and regulating water redistribution process (Zhou et al., 2019;Zhang et al., 2018). Some researchers suggest that vegetation retains water in shallow root layer, but consumes more soil water to survive (Cheng et al., 2020a;Wei et al., 2019). The increase of vegetation also increases evapotranspiration (ET) (Bai et al., 2020), thereby reducing runoff and soil water storage (SWS) (Wang et al., 2020a;Bai et al., 2020). Researches also have shown that vegetation restoration can increase regional precipitation (Yang et al., 2018;Feng et al., 2018). Some scholars state that vegetation restoration does not reduce the water resources amount in a region, but instead changes the distribution of water resources there (Su and Shangguan, 2019;Chen et al., 2020). Under the background of global climate change, hydrological cycle and its interrelationship with artificial vegetation restoration cannot be ignored (Li et al., 2018). In Mu Us Sandy Land (MUSL), a typical semi-arid region in 3NSP, vegetation restoration reshapes the hydrological cycle and causes the decline of groundwater level and the death of some reconstructed vegetation, making the research on hydrological cycle in this region particularly important for assessing the water resources (Meng et al., 2020;Zhao et al., 2019). Some researches attempt to quantify the impacts of afforestation and climate change on the hydrological cycle in the region, but there is little information about the overall distribution of water resources from top of the canopy to the bottom of the root zone in this region (Wang et al., 2020b).

Forest ecosystems are vital to our planet, like fixed carbon, and forest ecosystems in Northwest China can suppress wind erosion and fix sand (Piao et al., 2020). Most of the forests in the 3NSP are rain-fed forest(Cheng et al., 2021b), thus whether the precipitation can supply the survival of reconstructed PSM and the precipitation redistribution in shallow soil layer is important in this rain-fed forest ecosystems, which affect the water balance of forest land and the biochemical cycle

of this region. Precipitation flow through the canopy to form throughfall(Marin et al., 2000).

70 Throughfall and stem flow can reach the surface soil layer, recharge soil moisture, and eventually

are utilized by plant roots. Due to the importance and complexity of precipitation interception, a

large number of previous studies have been carried out on this subject for decades (Helvey and

Patric, 1965;Cheng et al., 2021a), but there are relatively few studies concerning precipitation

redistribution from atmospheric water to groundwater in rain-fed forest ecosystem such as 3NPS

75 in arid and semi-arid regions (Zheng et al., 2018). Among those limited studies in arid and semi-

arid regions, shrubs are usually the concern rather than trees, which are not native to this region

(Zhang et al., 2015), and the tall branches and broad root system of trees make them difficult to

carry out the controlled field-scale experiments.

After the successful introduction of Pinus sylvestris var. mongolia (PSM) in MUSL, more and

80 more attention has been paid to its excellent characteristics of drought resistance, barren resistance

and strong adaptability(Gao and Huang, 2020). PSM has become the most widely planted tree

species in northern sandy areas of China include MUSL, and it has played an important role in

controlling the expansion of sandy land. However, since the 2000s, PSM plantation in MUSL have

shown signs of degradation. Moreover, PSM forest in MUSL cannot reproduce, thus its

85 adaptability has been questioned by the academic community. Some researchers state that the

decrease in precipitation is the main reason for its degradation (Guo et al., 2020), but there are also

studies showing that precipitation actually increases after vegetation restoration in this region (Yan

et al., 2015). Indeed, there are few studies on precipitation redistribution of PSM forest, and it is

crucial to carry out such researches in the forest land of PSM vegetation restoration in MUSL to

90 better manage the forest land of PSM.

The scientific community generally agrees that vegetation restoration has changed the

redistribution process of precipitation resources, but the amounts of atmospheric water, soil water, plant water and groundwater transformed from precipitation have not been quantified accurately(Yu et al., 2018). Instead, previous studies have focused on the process of ground water

95 distribution rather than the overall distribution of precipitation (Dekker and Ritsema, 1994;Maxwell et al., 2007). The purpose of this study is to find out the effect of rain-fed PSM on precipitation redistribution in MUSL through in-situ observation experiments. Based on the analysis of the collected dataset, we hope to answer the following questions: Can precipitation recharge groundwater after PSM restoration? What are the proportions of evapotranspiration, SWS

100 and groundwater on precipitation? Can rain-fed PSM survive under existing annual precipitation conditions? To answer above problems, we have designed a comprehensive observation experiment system through continuous observation of precipitation redistribution process in PSM forest land and bare sandy land (BSL) in the northeastern MUSL. We try to understand the precipitation redistribution mechanism of PSM replantation and provide a theoretical basis for

105 managing sand-fixation plantation in MUSL. We will also try to exam whether the incapability of PSM reproduction is caused by water shortage. The knowledge gained from this investigation can provide insights for vegetation restoration and desertification control in northern China or similar regions in other parts of the world.

2 Material and methods

110 ### 2.1 Study area

The study area is located in Taigemiao (39°10′13.62″N, 109°31′51.59″E) on the northeastern of MUSL. MUSL is one of the severe desertification areas in China, thus a large area of vegetation restoration has been carried out since 1978. The reconstructed tree species include PSM, Salix psammophilous and Artemisia annua. PSM was planted in belts, with a row spacing of 20 meters.

115   This area belongs to typical semi-arid sandy region with dry climate with an average annual

temperature of 6.2 °C and a soil freeze-thaw period of about 150 days. The multi-year average

annual precipitation is 358.2 mm. The groundwater depth in the study area is 5-8 m, and varies

with seasons.
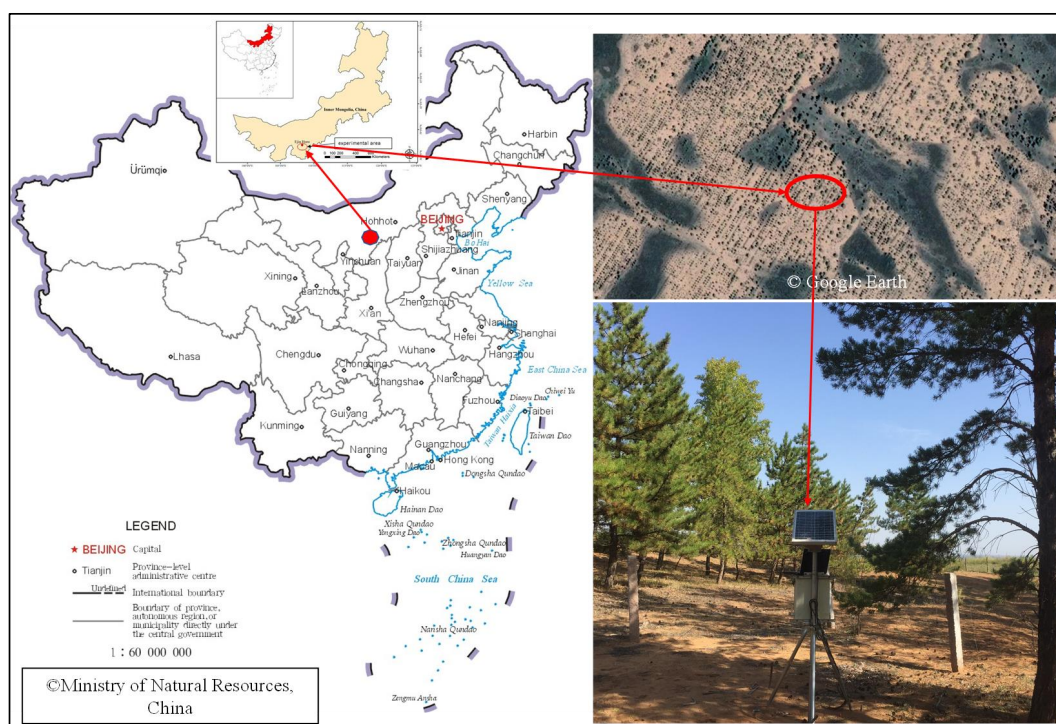
120   Figure 1 Location of research region, the red dots represent BSL plot, and the blue dots represent

PSM plot.

The source of groundwater recharge entirely come from precipitation in this region. The annual

precipitation distribution is uneven, with summer (June to August) accounting for more than 70 %

of the annual precipitation, and spring (March to May) accounting for only 10 % of the annual

125   precipitation. Annual potential evaporation is 2200 mm in bare sandy land (BSL). The main soil

type is aeolian sandy soil with a clay content of 0.83%, a silt content of 8.21%, a sand content of

90.96%, and an organic matter content of 2.0 ~ 3.5 g · kg^{-1} (Cheng et al., 2020c;Cheng et al., 2020a). The revegetation of PSM started in 1987, and the planting density was 1200 plants / ha. To compare the characteristics of precipitation redistribution after restoration of PSM, we decide

130   to select a BSL plot about 200 meters from PSM forest plot as a comparison and have used the same experimental setup in the PSM forest plot to monitor the redistribution process of precipitation as in the BSL plot. The location of the experimental site is shown in Figure 1.

2.2 Research method

To explore the distribution characteristics of precipitation in the reconstructed forest land, we

135   assume that the reconstructed forest land belongs to a relatively uniform landform system, thus we can select a typical sample plot from this system for observation (Taigemiao experimental plot). The landform in our study area is flat sandy land, as shown in Figure 1, PSM was planted in this area 30 years ago in belts, and the distance between the two belts was 15 meters. Under this uniform distribution of PSM forest land, it would be convenient to choose a PSM plot to

140   monitoring precipitation redistribution process along the vertical direction instead of studying the entire region, which is difficult or even impossible.

To study the redistribution characteristics of PSM forest land in Taigemiao experimental plot of MUSL, we set up an *in situ* observation system to observe the precipitation distribution in canopy interception, surface runoff, SWS, DSR and sap flow. Since 2015, the experimental field has been

145   established. As the installation of the instrument will inevitably cause soil disturbance, we irrigate the sample plot after the instrument installation to promote soil layer settlement. The observation data were collected a year later, from 2016, and the water distribution of precipitation in the atmosphere, soil layer and DSR are recorded and analyzed.

DSR is an important factor for regional water balance research, thus we will use a newly designed
150   lysimeter to measure DSR. As shown in Figure 2, the water source of PSM in MUSL is mainly
atmospheric water, the PSM has developed a shallow root system parallel to the ground surface to
maximize the area to intercept the precipitation-induced infiltration.   We have excavated and
flushed the experiment plot to exam the root system distribution and found that the roots of PSM
evenly distributed in the open space between the two PSM rows. The root distribution depth is
155   concentrated at 80 cm depth, and few roots can reach 100 cm depth. The capillary water holding
height of sandy soil in this area is 80 cm. Therefore, we decide to lay the newly designed lysimeter
at the depth of 200 cm, which include a 100 cm of root system, a capillary water rise height of 80
cm and additional 20 cm. Such an installation depth can ensure that the measured DSR will not
absorbed by the plant root system. Although soil vapor flow may exist in sandy soil, particularly
160   at shallow depths, the effect of soil vapor flow is regarded as secondary in this investigation. In
the future, soil vapor flow sensors are probably needed to quantify the exact nature of vapor flow.
By measuring the DSR and the water content of each soil layer, we can calculate
evapotranspiration.

The schematics of the newly designed lysimeter schematics is shown in Figure 2B. The traditional
165   lysimeter measuring face is at the ground surface and the measuring depth equals to the height of
the instrument. The newly designed lysimeter can be installed at any depth, depending on the site-
specific requirements. This instrument has two parts, an upper water balance part and a lower
measuring part. The balance part has a cylinder with an upper opening and a filter mesh at the
bottom. The filter mesh allows soil water to permeate but no soil particles can pass through. The
170   height of the balance part is equal to the height of capillary rise of the in-situ sandy soil. As shown
in Figure 2B, when the soil at layer B is saturated, the soil water can rise to layer A because of the

capillary force, but it would not overflow the cylindrical barrel, so as to reach a state of equilibrium. When the upper layer A has moisture infiltration, the moisture balance state is broken, and the excess water will be discharged from layer B into the measurement part. The measurement section uses a tipping bucket water meter to automatically record the infiltration rate. This is the principle of the newly designed lysimeter.

It is necessary to reduce the damage to the in-situ soil layer structure when installing the lysimeter. As the PSM root system is evenly distributed in the open space of the forest belt, we decide to excavate a soil profile in the middle of the PSM forest to install the lysimeter. The sand structure is relatively loose and easy to collapse. Therefore, before excavation, we need to irrigate the plot to reduce the risk of soil collapse during the instrument installation process. After irrigation, we will excavate a vertical soil profile in the middle of the forest belt. As the height of the instrument is 120 cm and the measuring surface depth is 200 cm, so we need to excavate a soil profile of 320 cm deep. After reaching a depth of 320 cm, we continue to excavate 100 cm in a direction parallel to the forest belt at the bottom of the profile, with a vertical cross section equaling to the side area of the new lysimeter, 30 cm by 120 cm. This will ensure that the soil layer on the upper part of the instrument would remain undisturbed as much as possible. After this, soil moisture probes are installed at targeted depths, as shown in Figure 2. Using the in-situ soil to backfill the excavation and irrigating the soil profile to facilitate the soil settlement, the installation procedure is then completed. It takes a certain time for the soil to settle down, so we need to install the instrument six months to one year in advance for the soil profile to settle down to its pre-excavation stage. After that, the data are collected automatically in a time series fashion.
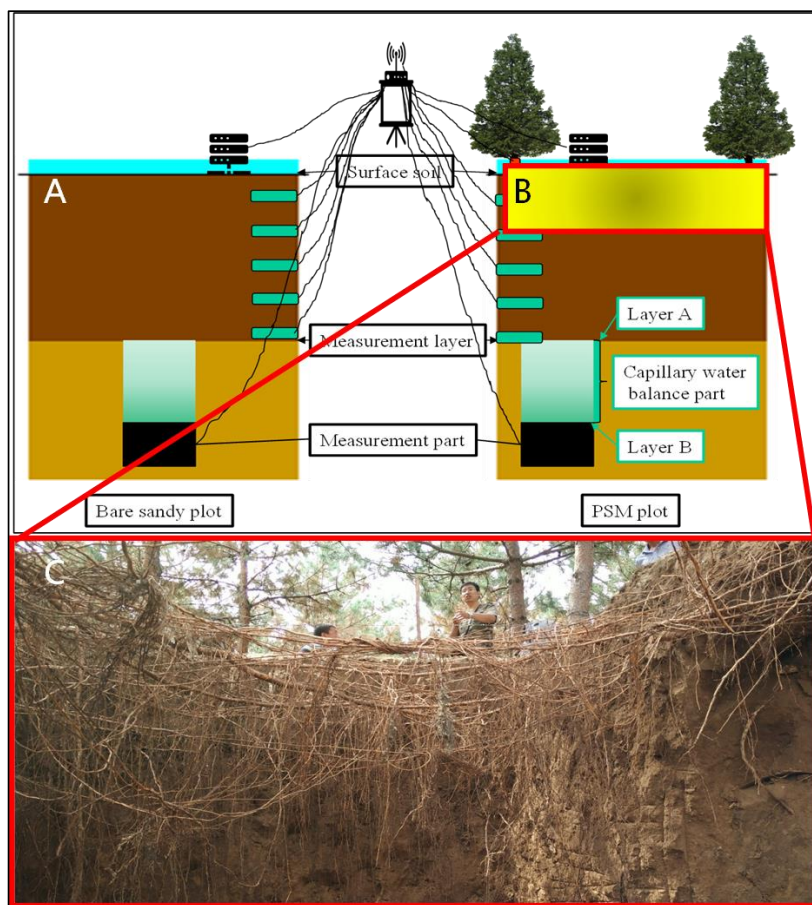
Figure 2 Schematic diagram of in-situ observation instrument installation, PSM plot and control
group BSL plot. A is the BSL plot, B is the PSM plot, C is the distribution characteristics of
PSM roots planted in the experimental field. (Fig C adapted from Dang et al., 2021)

2.2.1 Determination of sap flow

The sap flow flux equal to the transpiration of PSM. To determine the transpiration of PSM, we
have carried out the sap flow measurement of PSM. The planting years of PSM in this region are
the same, but the growth is not the same. However, it is impractical to monitor the sap flow of all
PSM. To obtain the transpiration of PSM forest in this region, we need to select a representative

PSM in the study area for observation. We measured the diameter at breast height (DBH) of PSM

in the study area, looking forward to screening suitable samples from the growth state. The

restoration of PSM plantation was planted according to the row belt. We selected 10 rows of PSM

205 with relatively uniform growth to measure DBH (500 columns). The average diameter of PSM

was 189.5 mm, and the median DBH of PSM was 191 mm, showing that the median and average

of PSM were quite similar to each other. Therefore, we selected the median DBH of PSM as the

observation objective of sap flow. FLGS-TDP plant sap flow meter (Dynamax, USA) was used to

measure and calculate the sap flow rate.

210 We install the sap flow instrument at the breast height of the PSM, this instrument composed of

two cylindrical probes with a diameter of 2 mm. These two probes were inserted up and down

along the growth direction of the stem, 2 cm depth into the sapwood with an interval of 10 cm.

The lower probe contained a heating element to heat the probe continuously. Each probe contained

a thermocouple to measure the temperature at any moment. The temperature difference between

215 these two probes was influenced by the stem sap flux rate. As the sap flow went upward, the

temperature difference between the two probes decreased. Therefore, by monitoring the

temperature difference between the two probes one can calculate the sap flow rate (Granier, 1987).

Previous experiences have shown that in northern China, the average flow rate of the whole tree

can be estimated with high precision using the flow rate on the northern side of the trunk of PSM

220 through a simplified model as follows:

$$V = 0.0119\ K\text{-}1.231 \times 3600,\ K = (dTm - dT)/dT \tag{1}$$

where V is the sap flow rate (cm·hr^{-1}), dTm is the maximum temperature difference between the

heating probe and the reference probe when there is no sap flow, and dT is the temperature

difference between the heating probe and the reference probe when sap flow occurs at any given

225   moment. The total volume of sap flow (F) was:

$$F = \sum_{i=1}^{n} V_i \times A_s \times \Delta t \tag{2}$$

where F was the total volume of sap flow (cm^3); n was the number of sampling; V_i was the sap

flow rate during the i-th sampling time interval (cm*hr^{-1}); As was the area of sapwood (cm^2), and

it was 196.755 cm^2; Δt was the sampling interval (hr).

230   ### 2.2.2 Soil water storage measurement

SWS came from precipitation infiltration and it was the most important water source for vegetation

in semi-arid areas. As there was no surface runoff in the experimental plot during the observation

period (2016-2019), the precipitation will contribute entirely to SWS after subtracting the

evaporation component. To maximize the contact area with shallow soil moisture, PSM roots grew

235   preferably along the horizontal direction rather than along the vertical direction. The vertical

distribution of PSM roots in MUSL was concentrated in the depth range of 0-200 cm, which also

suggested that PSM mainly used precipitation rather than groundwater as its water supply (Cheng

et al., 2021b). The SWS in this plot was calculated by measuring the volumetric water content and

soil thickness of each layer where the soil volumetric water content was measured by the EC-5

240   (resolution: 0.1 % VWC, METER Environment, USA) soil moisture sensor. The measurement

range was the top 200 cm soil layer, and soil moisture probes were installed at 20, 40, 60, 80, 120,

160 and 200 cm depths below the ground surface, and the SWS was calculated as follows:

$$SWS = \sum SWS_i \tag{3}$$

$$\Delta SWS = \sum SWS_{t1} - \sum SWS_{t2} \tag{4}$$

245   where *SWS* was the soil water storage of the entire soil layer, ΔSWS was the change value of *SWS*

from t_1 to t_2. In this research, ΔSWS refers to the difference between the $\sum SWS_{t1}$ at the end of the

experiment in November and the $\sum SWS_{t2}$ at the beginning of the experiment in March.

2.2.3 Measurement of deep soil recharge

DSR refers to the infiltration of precipitation into the soil layer at a certain depth (Cheng et al.,

250   2017b), it is expected that precipitation infiltrated to this depth soil layer will not be absorbed by

the roots or return to atmosphere via evapotranspiration. Strictly speaking, it was possible for soil

water in any layer to return to atmosphere through the evapotranspiration process with either liquid

or vapor phase flows(Wei and Dirmeyer, 2019;Cahill and Parlange, 1998). However, the soil water

at a capillary holding height depth below the root layer was not easily absorbed by the roots or

255   volatilized in the form of water vapor. Therefore, vapor flow was regarded as a secondary effect

ad was not taken into consideration in this investigation. In the future, vapor flow sensors will be

installed in the site to investigate the vapor flow dynamics. DSR was an important indicator for

several processes. For instance, it could tell if the precipitation infiltration in the region was

sufficient to sustain the growth of plants or not. More specifically, if DSR could be detected, it

260   indicated that the precipitation infiltration could meet the needs of growth of plants, with some

extra water available for recharging the deep groundwater below the root zones. On the other hand,

if there was no detectable DSR, it suggested that the precipitation infiltration was probably not

sufficient to meet the consumption of plants in the region.

Despite of its obvious importance, it was generally difficult to measure DSR directly and there

265   were very few studies on this matter up to present. To resolve this issue, our research team has

designed, installed, and tested a field-based and inexpensive DSR measurement instrument, as

shown in Figure 2 (Cheng et al., 2018). The use of this instrument (DSR, measurement accuracy:

0.2 mm, China) for the measurement of DSR has been verified in several previous studies(Cheng

et al., 2020a;Cheng et al., 2020b).

270   ## 3 Results

The in-site experimental instruments recorded the distribution of precipitation in atmosphere (ET),

shallow soil layer (SWS) and groundwater (DSR) from 2016 to 2019. ET was calculated by the

water balance equation, and results were shown in Table 1. The 30-year annual average

precipitation in the Taigemiao was 358.2 mm. We defined the year with a precipitation amount

275   higher than the multi-year average precipitation as a wet year, and the year with precipitation lower

than the multi-year average precipitation as a dry year.

3.1 Statistics of precipitation redistribution process

As shown in Table 1, the annual precipitation in 2016 reached 506.4 mm, indicating a wet year.

The precipitation in this year deviated about 41.37 % from the average annual precipitation. It is

280   worthwhile to point out that average annual precipitation may not be a good indicator for the actual

precipitation state in the site, as extreme precipitation events occurred frequently in this region.

Precipitations in the other three years of 2017, 2018 and 2019 were less than the average annual

precipitation amount, indicating dry years. The precipitation in 2018 was only 239.8 mm, which

deviated from the average annual precipitation by a deficit of 33.05 % (the multi-year average

285   annual precipitation was 358.2 mm). Therefore, we needed to consider the growth prospect of

vegetation under extreme drought and wet conditions in the process of vegetation restoration. This

study focused on the distribution of precipitation in different parts in two extreme wet and dry

years (2016, 2018), respectively.

In 2016, the distribution ratios of precipitation in atmospheric water (ET), soil water and DSR in

290   the PSM plot were 92.2%, 7.5% and 0.3%, respectively. We found that ET accounted for most of

the precipitation, but one should be noted that the observed proportion of ET in precipitation was

likely to be larger than the true value. This was because PSM not only consume soil moisture

contributed from precipitation of 2016, it could also consume the residual soil moisture coming

from precipitations of previous years such as 2015. The distribution ratios of precipitation in BSL

295   in atmospheric water, soil water and DSR were 27.1%, 18.9% and 54.03%, respectively. A

comparison of PSM and BSL plots in 2016 revealed that vegetation restoration has considerably

changed the distribution of precipitation in this region in at least two ways. Firstly, atmospheric

water increased considerably. ET increased because of the presence of vegetation. In 2016, ET in

the PSM plot was 2.35 times higher than that in the BSL plot (Table 1). Secondly, in 2016, SWS

300   of the PSM plot increased 38.06 mm and that of the BSL plot increased 95.67 mm, whereas SWS

of the PSM plot decreased by 60.2%. Therefore, we could conclude that vegetation restoration

significantly changed the distribution of precipitation in shallow soil. Precipitation was largely

converted into groundwater in the BSL plot, while precipitation was intercepted in shallow soil,

and large amount of precipitation converted to ET in the PSM plot.

305   Table 1 Table of precipitation redistribution in the ET, SWS, DSR, etc. on the plots

Time	Plot	Precipitation (mm)	Sap flow (mm)	ΔSWS (mm)	DSR (mm)	ET (mm)	T (mm)	E (mm)	DSR/P (100%)
2016	PSM	506.4	144.12	38.06	1	466.94	322.82	144.12	0.20
	BSL	506.4	-	95.67	273.6	137.13	137.13	-	54.03
2017	PSM	309	165.43	-16.00	0.2	324.60	159.17	165.43	0.06
	BSL	309	-	61.89	67.7	179.41	179.41	-	21.91
2018	PSM	239.8	90.51	54.75	1.2	183.85	93.34	90.51	0.50

	BSL	239.8	-	96.8	55.2	87.8	87.8	-	23.02
2019	PSM	341.6	152.39	-7.58	0	349.18	196.79	152.39	0.00
	BSL	341.6	-	64.38	124.9	152.32	152.32	-	36.56

2018 is an extremely dry year (with an annual precipitation of 239.8 mm), which deviated from the multi-year average precipitation by 54% (the multi-year average annual precipitation was 358.2 mm). The distribution ratios of ET, SWS and DSR in the PSM plot were 76.7%, 22.8% and 0.5%,

310 respectively in 2018, indicating that ET still accounted for most of the precipitation in that year. The distribution ratios of atmospheric water, SWS and DSR in the BSL plot were 36.6%, 40.4% and 23%, respectively in 2018. A comparison of the data for the PSM and BSL plots revealed that DSR of the BSL plot was larger than ET, and 23% of the precipitation recharged the deep soil layer or groundwater in the BSL plot in 2018. Precipitation was intercepted in the shallow soil

315 layer in the PSM plot. In 2018, only 0.5% of precipitation was involved in recharging the deep soil layer or groundwater in the PSM plot. These results again suggested that whether in dry or wet year, the PSM forest has substantially changed the redistribution of precipitation.

As shown in Table 1, precipitation, sap flow, SWS and DSR varied greatly during the observation period of 2016-2019. Traditional studies used a coefficient to determine the amount of DSR was

320 found to be questionable, as indicated by Cheng et al. (2017a). Here we applied the Pearson correlation method to analyze the correlation between precipitation and sap flow, SWS, DSR, ET, evaporation (E) and transpiration (T) during the study period (Table 2). In the PSM plot, precipitation was closely correlated with ET (P = 0.99706), indicating that the increase of precipitation directly promoted the increase of ET. On the other hand, there was no direct

325 correlation between sap flow and precipitation.

As shown in Table 1, the variations of sap flow in 2016, 2017 and 2019 were much smaller than the variations of precipitations in these years, suggesting that once vegetation in semi-arid areas adapted to the environment, sap flow (transpiration) remained relatively stable despite changes in annual precipitation. Furthermore, we can see that the evaporation is positively correlated with the

330   precipitation, meaning that the increase in precipitation will not cause a sudden increase in transpiration, but it will cause an increase in evaporation. Such a correlation indicated that we could infer whether a plant was under drought stress or not by measuring the sap flow and then determining whether the observed value was lower than the average value. The PSM sap flow decreased considerably in 2018 (because that is an extremely dry year), indicating that PSM was

335   under drought stress by extreme drought years such as 2018. In future vegetation restoration activities, attention should be paid to reducing the planting density of PSM to adapt to climate change in this area. In contrast, there was no interference of vegetation transpiration in BSL. DSR was found to be closely correlated with Precipitation with a Pearson coefficient of 0.9797. The correlation between precipitation and evaporation was not significant (with a Pearson coefficient

340   of 0.27416). This finding showed that the evaporations of both the PSM and BSL plots did not change considerably after the vegetation restoration, suggesting that vegetation restoration did not reduce surface evaporation.

Table 2 Correlation analysis of precipitation and each part water distribution amount

Pearson correlation analysis	Plot	Sap Flow	SWS	DSR	ET	E	T
Precipitation	PSM	0.4428	0.0594	0.08953	0.95364	0.99706	0.4428
	BSL	-	0.22671	0.9797	0.27461	0.27461	-

3.2 Sap flow characteristics

Sap flow could be used to directly determine whether an area was under drought stress or not. In this study, we used the TDP to measure sap flow where the TDP sap flow meter adopted the principle of thermal diffusion. Specifically, we combined the measured sap flow of PSM with the measured sapwood area to estimate the evaporation. In this study, we monitored DSR, precipitation and SWS through the water balance equation: $P = ET + SWS + DSR$. The ratios of ET/P, SWS/P, and DSR/P were estimated for both the PSM and BSL plots and the results are shown in Table 1. For the PSM plot, the ET value included transpiration and evaporation, and transpiration was calculated from the sap flow measurements taken with the TDP sap flow meter. For the BSL plot, the ET value only included evaporation as there was no transpiration when PSM and other plants were absent.

The sap flow usually started in early March and ended in October during the four-year period of investigation. As shown in Fig. 3a, the sap flow curve had two peaks, the first in June and the second in August. Because 2016 was a wet year, the precipitation in July was relatively high, and the sap flow was low during the precipitation period. This suggested that the sap flow rate during a specific precipitation event might be suppressed by that event, but overall, why was there no significant change in the annual sap flow rates for the wet year (like 2016) and dry year (like 2019)? Recent studies have shown that rising temperatures caused by increasingly strong solar radiation can keep plants transpiration even at night (Panwar et al., 2020). The short duration of precipitation in this region may be the reasons for little change in the annual sap sap flow amount, which was related to the annual net radiation amount.
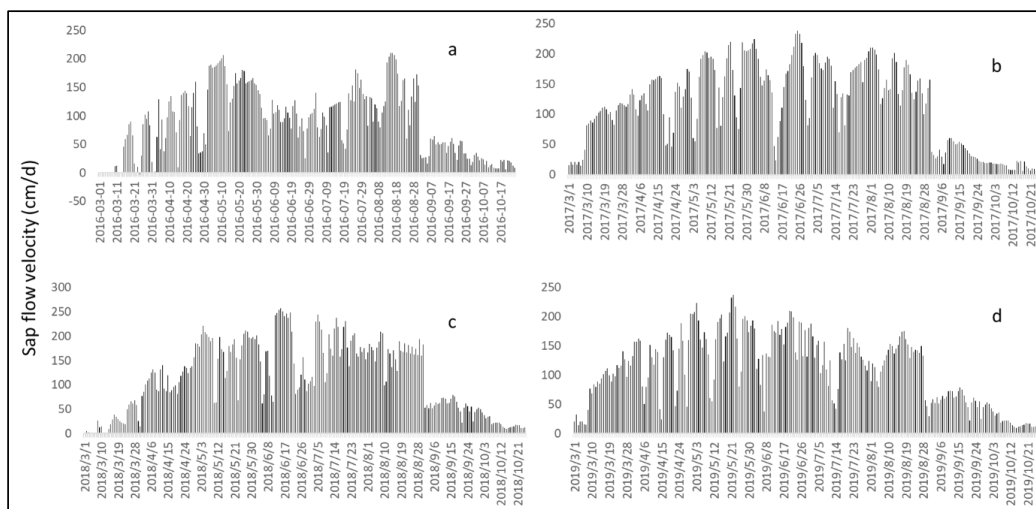
Figure 3 Annual variations of DBH sap flow on the north side of PSM, 2016-2019

As shown in Fig. 3, solar radiation significantly decreased then the sap flow decreased after
September 7. In drought years, the maximum sap flow rate appeared from June to July with only

370   one peak, as shown in Fig. 3(b–d). It should be noted that only one sap flow data point with the
median DBH in this study (we have only one sap flow instrument) was measured and this PSM
was used to represent the average transpiration for all PSM forest land in this area. The PSM forest
land in the experimental area was evenly distributed and there was no competition between
adjacent trees. Thus, there was no difference in sap flow rates among dominant trees, medium trees

375   and inferior trees. The four-year measurements of sap flow indicate that there was usually no direct
relationship between annual sap flow and precipitation (except for extreme drought years like
2018).

3.3 SWS characteristics

SWS was calculated according to the soil volumetric water content of each soil layer and soil depth.

380   The accuracy of the soil moisture sensor (EC-5) decreased during the freeze–thaw period, thus we

selected the soil moisture data from March to October for the calculation of SWS in this study. We calculated the annual changes in SWS in for the four years, as shown in Table 1. To compare the differences in SWS changes between dry and wet years, we selected SWS in a wet year (2016) and a dry year (2019) to conduct a more detailed comparison.

385   As shown in Table 1, SWS of the PSM plot in 2016 increased by 38.06 mm, and that of the BSL plot increased by 95.67 mm. The daily accumulations of SWS in these two plots are shown in Figure 4. Figure 4a shows daily change of SWS in the PSM plot in 2016. The PSM plot only shows one period with negative values of SWS (June 18–28), with positive values for the rest of the year. The annual SWS of the BSL plot was positive, reaching 95.67 mm. The variation of SWS varied

390   between these two plots. Before the rainy season, SWS in the BSL plot was smaller, whereas SWS in the PSM plot was larger. Considering that PSM was in a dormant state and did not consumed soil water at this stage, the SWS capacity of the PSM plot was considerably improved after vegetation restoration. Related studies have also shown that soil texture was improved after vegetation restoration. The maximum daily SWS in the PSM plot was 260 mm, whereas that in

395   the BSL plot was 197 mm.
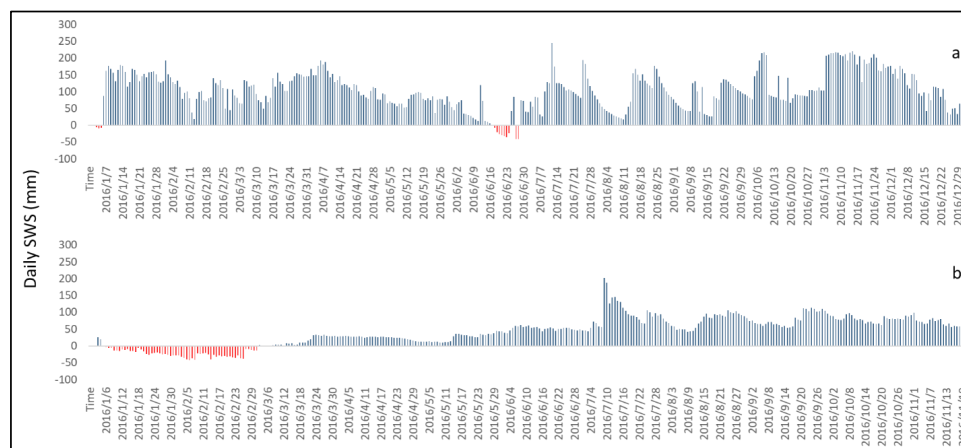
Figure 4 Daily cumulative SWS in PSM plot (a) and BSL plot (b) in 2016.

Annual precipitation in 2019 was 341.6 mm. In the PSM plot, the annually changed value of SWS

was −7.58 mm in 2019, indicating that PSM consumed SWS to survive under these precipitation

400   conditions. The DSR was 0 mm, indicating that there was no precipitation-induced infiltration

penetrating the shallow soil layer, and precipitation was completely intercepted by PSM. The SWS

in BSL was 96.8 mm and DSR was 55.2 mm, and the distribution ratio of precipitation varied

considerably among the two plots in 2019. Taking the BSL plot as an example, SWS was high

before the freeze–thaw period (November 2019) and low after the freeze–thaw period (March

405   2020). Moreover, SWS changed during freeze–thaw, suggesting that water vapor flow might be

involved during the freeze–thaw period. Because of the decrease of sensor accuracy in winter, we

were unable to quantify the SWS change during the freeze–thaw period. The amount of DSR in

the BSL plot was much greater than that in the PSM plot. The ratio of DSR over precipitation

reached 37.7%, indicating that a relatively high proportion of precipitation was employed in

410   groundwater recharge before PSM restoration.
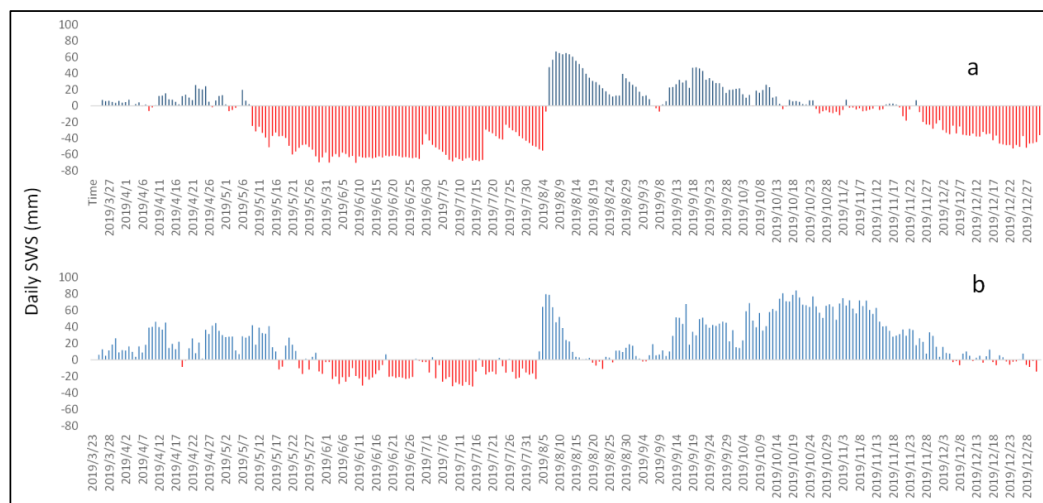
Figure 5 Daily cumulative SWS in PSM plot (a) and BSL plot (b) in 2019

To explore the daily change of SWS, we considered the SWS changes in 2016 in more detail.
Because 2016 was a wet year, there were more precipitation events available for comparison. As
415   shown in Fig. 6a, the SWS increased rapidly after precipitation, and SWS was consumed after
precipitation. As shown in Fig. 6(b–d), SWS changed from positive to negative after precipitation
because of vegetation transpiration and surface evaporation. The attenuation characteristics varied
among different seasons. In the two precipitation-evapotranspiration events in the growing season,
the SWS returned to 0 mm on 7 days after the cessation of one precipitation event in July and
420   August, but returned to 0 mm on 12 days after the cessation of one precipitation cycle in September
(Fig. 6b, c). The soil evapotranspiration maintained a relatively constant rate after the precipitation
events in September (Fig. 6d). The main factors affecting soil water storage in summer were
transpiration and evaporation, whereas in autumn, transpiration reduced and only evaporation
prevailed. We speculated that PSM had entered the dormancy period in late September, although
425   the soil layer had not entered the freeze–thaw period at that time.
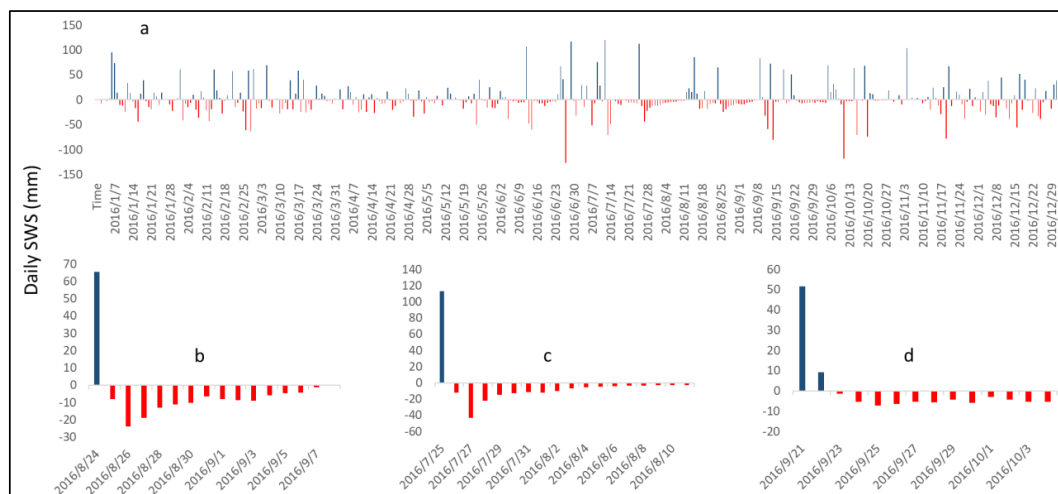
Figure 6 Daily variation of SWS in PSM plot and the change of SWS in different months, 2016

3.4 Characteristics of DSR

The DSR was determined by using the newly designed lysimeter (Table 1). The DSR values in the

430   PSM plot were only 1, 0.2, 1.2 and 0 mm in 2016, 2017, 2018 and 2019, respectively, whereas

those in the BSL plot were 273.6, 67.7, 55.2 and 124.9 mm, respectively. The greatest change in

the process of precipitation redistribution after vegetation restoration was that of DSR, which

directly affects groundwater recharge in this region. In the dry year (2018), DSR decreased by 54

mm, and in the wet year (2016), DSR decreased even more. This suggests that continued large-

435   scale afforestation in this area will cause the interruption of groundwater recharge in MUSL.

In 2016, only 1 mm DSR occurred in the PSM plot, mainly from September 18 to September 20.

According to Figure 6d, even in wet years like 2016, precipitation in the PSM plots could not fully

recharge groundwater. By September, the sap flow decreased sharply (Fig. 3a). Without the PSM

interception, a small amount of precipitation was able to penetrate the shallow soil layer to become

440   DSR.
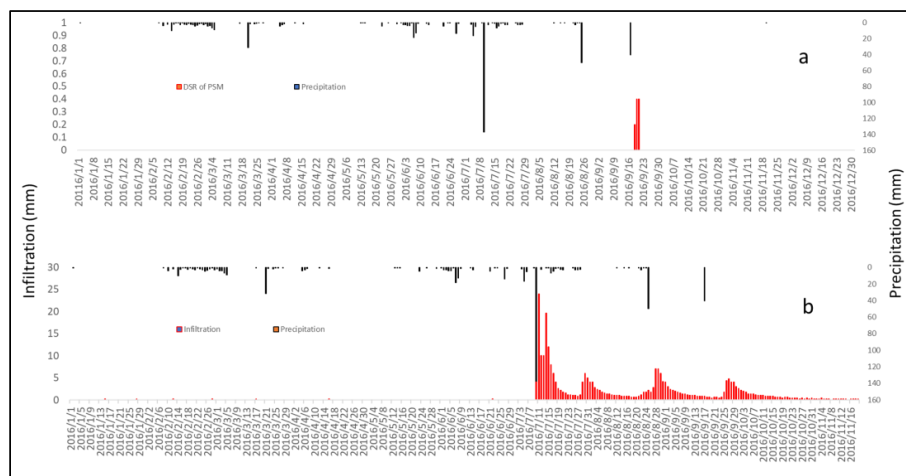
Figure 7 The relationship between precipitation and DSR, (a) was daily scale precipitation and

infiltration in PSM plot, (b) was daily scale precipitation and infiltration in BSL plot.

The rate of DSR varied among different seasons. As shown in Fig. 7b, a precipitation event on

445 August 25 reached 50 mm, and 48 hr later, the precipitation-induced infiltration had reached 200

cm soil depth to become DSR. On September 17, daily precipitation reached 40.2 mm, and 168 hr

later, the precipitation-induced infiltration reached 200 cm soil depth to become DSR. The main

difference between these two precipitation events was soil temperature. Therefore, understanding

the soil temperature impact on DSR appeared to be relevant and should be considered in future

450 investigations. Previous studies have suggested that the main factors affecting infiltration were the

initial soil moisture and precipitation intensity. In the current study, we found that soil temperature

also profoundly affected the infiltration rate. A comparison of DSR values in the PSM and BSL

plots reveals that the infiltration signal at 200 cm soil depth in the PSM plot was observed 24 days

after the precipitation event, whereas the infiltration signal in the BSL plot was observed 2 days

455 after the same precipitation event, indicating that the existence of PSM slowed down the

infiltration rate substantially, as the infiltration rate in the BSL plot was nearly 11 times faster than

that in the PSM plot.

4 Discussion

The soil layer carried the vast majority of terrestrial ecosystems, and soil water played an important

460 role in the water cycle between land surface, atmosphere and groundwater, which was the main

role in the water balance of the earth system (Bastin et al., 2019). The concept of the soil–plant–

atmosphere continuum (SPAC) has been formed from the perspective of water redistribution

(Manzoni et al., 2013). Water was an important component in the SPAC system and the soil–

vegetation–atmosphere transport (SVAT). Based on these theories and associated models (Franks

465 et al., 1997), researchers have gradually developed a model of the earth system that quantitatively

describes the feedback of land surface processes in the climate system (Foley et al., 1996). The

characteristics of soil moisture on climate anomalies were the most important processes affecting climate change, except for the ocean (Entekhabi et al., 1996). However, because of the limitations of experimental observation conditions, and large-scale ecological restoration projects were far beyond the imagination of scientists, the redistribution process of precipitation in artificial forest land had not attracted enough attention. In particular, how the change of surface vegetation cover affected the groundwater recharge, and ecosystem degradation caused by massive vegetation restoration have not yet been quantitatively described.

The impact of ecosystem degradation on biodiversity and climate has promoted the grand goal of ecosystem restoration at all levels in various countries around the world (Ortiz et al., 2021). The United Nations announced 2021–2030 as the "United Nations ecosystem restoration decade", and the "Bonn challenge" and "New York Forest Declaration" aim to restore 350 million hectares of global forest by 2030(Zhao et al., 2020). There was no doubt about the carbon sequestration effect of forests, but vegetation restoration shows considerable regional variation (Harmon, 2001). China has implemented some large-scale afforestation plans in arid and semi-arid regions, including the northeast, north and northwest, to prevent desertification and control sandstorms(Cao et al., 2011). These vegetation restorations alleviated environmental problems such as desertification, which made the study of water resource redistribution in semi-arid areas more important. Some studies have criticized this process of vegetation restoration, arguing that vegetation restoration in semi-arid areas would aggravate ecological problems (Xiao et al., 2020;Fensholt et al., 2012). However, in our opinion, these projects have been carried out for 40 years and have achieved goals in most areas.

Research has shown that China's vegetation restoration has made certain contributions for increasing the forest cover in the world (Chen et al., 2019). Numerous research results have led to

490   discussions regarding the optimal ecological restoration process for China(Chen et al., 2019). The

uncertainty of vegetation restoration in China can ultimately be attributed to the question of

whether or not there was a water resources shortage (Cheng et al., 2021b). Many studies have

shown that vegetation restoration would increase precipitation and transpiration in the region

(Meng et al., 2020). Some studies on the Loess Plateau have shown that afforestation leaded to an

495   increase in ET and decrease in soil moisture and runoff (Zhang et al., 2018;Jia et al., 2017). These

studies also pointed out that revegetation might exacerbate the sustainability of water resources

management, especially water resource carrying capacity increased by human activity. These

studies have not specifically observed the distribution of precipitation in the atmosphere and its

redistribution to plant, soil and groundwater. In this study, we found that previous studies may

500   have underestimated the hydrological effects of vegetation greening and also underestimated the

capability of vegetation to redistribute precipitation (Cheng et al., 2017a). This leaded to

uncertainties in the question of how vegetation changed SWS and DSR during vegetation

restoration in MUSL.

Most previous studies used remote sensing method for analysis on a large regional scale, but they

505   could not provide sufficient specific experimental data for use in verification (Li and Pan,

2018;Gong et al., 2019). Moreover, remote sensing could not obtain deep soil moisture data, and

could not obtain DSR. Thus, it was impossible to determine the recharge effect of precipitation on

groundwater. Some studies focused on the measurement of a single factor, and cannot

systematically study the precipitation redistribution in the restoration process of PSM forest in

510   MUSL (Yu et al., 2018). In this study, most water redistribution factors (except soil vapor and soil

temperature effects) in the vertical direction of the reconstructed vegetation PSM forest land in

MUSL were monitored, and the factors from atmospheric water, plant sap flow to in situ

monitoring data were applied to consider the consequences of vegetation restoration. This study

has been carried out for 4 years so far, and continuous data collection must be carried out to

515   generate a long-term time-series dataset. In addition, we suggest the following areas for future

improvement in this study:

1. We could not measure the amount of vapor flow in the shallow soil layer. In semi-arid regions,

vapor flow was likely to vary greatly. We needed to install vapor flow sensors and introduce a

hydrothermal transport model considering the vapor flow component based on this observation in

520   the future.

2. Although we screened a typical PSM plot to represent the general water distribution state of

PSM in this region, our research was limited to the monitoring of a single experimental plot. Given

the goal of precipitation redistribution in the 3NSP region, we needed to develop larger-scale

observation plots in the future to assess the scale-sensitivity of trees, shrubs, grasslands and

525   farmlands across different precipitation gradients.

3. There was a freeze–thaw period up to 4 months in this region. In the freeze–thaw period, we

could not accurately observe the change of soil moisture. In this study, we chose to show the annual

soil moisture, because the thickness of freeze–thaw layer did not change substantially on a daily

scale, and the error of soil moisture could be ignored. However, in the analysis at annual scale, we

530   did not use the soil moisture during the freeze–thaw period. Based on the difference of SWS at the

end of one year and the beginning of the following year, we found that the soil moisture and DSR

changed in the freeze–thaw period. Therefore, it was necessary to study the soil moisture change

during the freeze–thaw season using an alternative method.

4. Existing studies have shown that vegetation restoration was conducive to the increase of

535   precipitation in the region, but our observations showed that precipitation in MUSL exhibited

significant fluctuations, to the extent that precipitation across most periods were considerably lower than the average precipitation across many years, suggesting that instability was likely in the future development of PSM in MUSL. To date, vegetation restoration has been carried out for 40 years. Although the vegetation coverage was relatively low in the early period and had little

540 impact on the environment, vegetation coverage increased from 5% to 15% between 1979 and 2020, research was needed to examine whether the regional precipitation intensity changes need to be considered in more detail or not.

5 Conclusions

This study focused on the redistribution of precipitation in the PSM and BSL plots through

545 observation of sap flow, SWS, DSR and annual precipitation in MUSL. In this study, we determined the threshold of precipitation distribution in each part and replenishment of groundwater and compared the characteristics of precipitation redistribution after vegetation restoration by comparative experiments. This study aimed to understand the redistribution process of precipitation in PSM restoration land, improve the understanding of rain-fed PSM degradation

550 and future management of plantations in MUSL. The PSM consumed soil water in the uppermost soil layers, which might impact the long-term sustainable development of PSM forest in MUSL and the decline of the groundwater level might cause an ecological crisis. Our specific conclusions were as follows:

1. MUSL has experienced 40 years of vegetation restoration. The PSM forest has considerably

555 changed the process of regional water redistribution. The most obvious change was the decrease of precipitation-induced recharge to groundwater. The DSR values were 273.6 mm in a wet year (2016) and 55.2 mm in a dry year (2018) in the BSL. The DSR value was only 1 mm in a wet year (2016) and there was no DSR in a dry year (2018) in the PSM plot. For the wet year (2016) in the

BSL plot, DSR accounted for 54.03% of the annual precipitation, whereas for the dry year (2018),

560   23.02% of precipitation was transformed to DSR in the BSL plot.

2. There was a clear relationship between evaporation and precipitation but transpiration was not correlated with annual precipitation. The surface evaporation of the PSM plot reached 322.82 mm in the wet year (2016), whereas that of the BSL plot was only 137.13 mm in the same year.

3. Through the measurement of sap flow of PSM, we found that sap flow of PSM remained

565   relatively stable (with a deviation of 153.98 mm/yr) except for the extreme drought year (2018, precipitation 239.8 mm, sap flow, 90.51 mm/yr), indicating that in MUSL, precipitation met the demand of PSM. However, in extreme drought years, the PSM entered drought stress and transpiration decreased, indicating that the cause of PSM degradation was the extreme drought conditions. Therefore, it was necessary to reduce PSM forest restoration density to allow

570   adaptation to extreme drought in the future.

4. The presence of PSM changed SWS. Compared with BSL, the SWS capacity of the PSM plot improved from 195 to 250 mm from 2017 to 2019, but due to transpiration by plants and soil evaporation, the SWS entered a deficit of 16 mm in 2017 and 7.58 mm in 2019. In the uncertain future under the influences of climate change, continuous drought may cause a water deficit in the

575   uppermost soil layers.

5. Vegetation restoration has changed the redistribution process of precipitation in this region. Due to the existence of PSM, the infiltration rate was significantly reduced, and the precipitation was intercepted in the shallow soil layer, then evapotranspiration increases, DSR significantly decrease.

580   **Declarations**

Availability of data and material: All the data are available from the corresponding author on reasonable request.

Competing interests: The authors declare that they have no competing interests.

Funding: This study was supported with research grants from the National Natural Science

585   Foundation of China (No. 41771306, No. 31971726, No. 41901234), National Key Research and Development Program of China (2019YFE0116500, 2018YFC0507100, 2019ZD003).

Authors' contributions: C.YB., W.B., J. QO., S. MC., B. XY., and Z.HB., conceived the idea; C.YB., W.B., and W.YQ., conducted the analyses; C.YB., provided the data; all authors contributed to the writing and revisions.

590   **Acknowledgements:** We gratefully acknowledge the Beijing Municipal Education Commission for their financial support through Innovative Transdisciplinary Program "Ecological Restoration Engineering". We thank the Desert Forestry Experimental Center of the Chinese Academy of Forestry for providing the experimental site. Thanks to the experimental site provided by Inner Mongolia Dengkou Desert Ecosystem National Observation Research Station, the Experimental

595   Center of Desert Forestry. Thanks to the Technical support provided by the key technology research and demonstration of the ecological and cultural industry in the Hunshandake Sandy Land. We gratefully acknowledge the Beijing Municipal Education Commission for their financial support through Innovative Transdisciplinary Program "Ecological Restoration Engineering".

600

Reference

[1] An, H., Wu, X., Zhang, Y., and Tang, Z.: Effects of land-use change on soil inorganic carbon: A meta-analysis, Geoderma, 353, 273-282, 2019.

[2] Azareh, A., Rahmati, O., Rafiei-Sardooi, E., Sankey, J. B., Lee, S., Shahabi, H., and Ahmad, B. B.:

605   Modelling gully-erosion susceptibility in a semi-arid region, Iran: Investigation of applicability of

certainty factor and maximum entropy models, Science of the Total Environment, 655, 684-696,

2019.

[3] Bai, P., Liu, X., Zhang, Y., and Liu, C.: Assessing the impacts of vegetation greenness change on

evapotranspiration and water yield in China, Water Resources Research, 56, e2019WR027019,

610   2020.

[4] Bastin, J.-F., Finegold, Y., Garcia, C., Mollicone, D., Rezende, M., Routh, D., Zohner, C. M., and

Crowther, T. W.: The global tree restoration potential, Science, 365, 76-79, 2019.

[5] Cahill, A. T., and Parlange, M. B.: On water vapor transport in field soils, Water Resources Research,

34, 731-739, 1998.

615   [6] Cao, J., Zhang, X., Deo, R., Gong, Y., and Feng, Q.: Influence of stand type and stand age on soil

carbon storage in China's arid and semi-arid regions, Land Use Policy, 78, 258-265, 2018.

[7] Cao, S., Chen, L., Shankman, D., Wang, C., Wang, X., and Zhang, H.: Excessive reliance on

afforestation in China's arid and semi-arid regions: lessons in ecological restoration, Earth-

Science Reviews, 104, 240-245, 2011.

620   [8] Chen, C., Park, T., Wang, X., Piao, S., Xu, B., Chaturvedi, R. K., Fuchs, R., Brovkin, V., Ciais, P.,

and Fensholt, R.: China and India lead in greening of the world through land-use management,

Nature sustainability, 2, 122-129, 2019.

[9] Chen, Y., Xu, M., Wang, Z., Chen, W., and Lai, C.: Reexamination of the Xie model and

spatiotemporal variability in rainfall erosivity in mainland China from 1960 to 2018, Catena, 195,

625   104837, 2020.

[10] Cheng, Y., Zhan, H., Yang, W., Dang, H., and Li, W.: Is annual recharge coefficient a valid concept

in arid and semi-arid regions?, Hydrology and Earth System Sciences, 21, 5031-5042, 2017a.

[11] Cheng, Y., Zhan, H., Yang, W., Dang, H., Li, W. J. H., and Sciences, E. S.: Is annual recharge

coefficient a valid concept in arid and semi-arid regions?, 21, 5031, 2017b.

630   [12] Cheng, Y., Li, Y., Zhan, H., Liang, H., Yang, W., Zhao, Y., and Li, T.: New comparative

experiments of different soil types for farmland water conservation in arid regions, Water, 10,

298, 2018.

[13] Cheng, Y., Li, X., Wang, Y., Zhan, H., Yang, W., and Jiang, Q.: New measures of deep soil water

recharge during the vegetation restoration process in semi-arid regions of northern China,

635   Hydrology and Earth System Sciences, 24, 5875-5890, 2020a.

[14]

[15] Cheng, Y., Yang, W., Zhan, H., Jiang, Q., Shi, M., and Wang, Y.: On the Origin of Deep Soil Water

Infiltration in the Arid Sandy Region of China, Water, 12, 2409, 2020c.

[16] Cheng, Y., Yang, W., Zhan, H., Jiang, Q., Shi, M., Wang, Y., Li, X., and Xin, Z.: On Change of Soil

640   Moisture Distribution With Vegetation Reconstruction in Mu Us Sandy Land of China, With

Newly Designed Lysimeter, Frontiers in Plant Science, 12, 10.3389/fpls.2021.609529, 2021a.

[17] Cheng, Y., Zhan, H., Yang, W., Jiang, Q., Wang, Y., and Guo, F.: An ecohydrological perspective of

reconstructed vegetation in the semi-arid region in drought seasons, Agricultural Water

Management, 243, 106488, 2021b.

645   [18] Dang, H., Han, H., Chen, S., and Li, M.: A fragile soil moisture environment exacerbates the climate

change-related impacts on the water use by Mongolian Scots pine (Pinus sylvestris var.

mongolica) in northern China: Long-term observations, Agricultural Water Management, 251,

106857, 2021.

[19] Dekker, L. W., and Ritsema, C. J.: How water moves in a water repellent sandy soil: 1. Potential and

650   actual water repellency, Water Resources Research, 30, 2507-2517, 1994.

[20] Deng, C., Zhang, B., Cheng, L., Hu, L., and Chen, F.: Vegetation dynamics and their effects on

surface water-energy balance over the Three-North Region of China, Agricultural and Forest

Meteorology, 275, 79-90, 2019.

[21] Doelman, J. C., Stehfest, E., van Vuuren, D. P., Tabeau, A., Hof, A. F., Braakhekke, M. C., Gernaat, D. E., van den Berg, M., van Zeist, W. J., and Daioglou, V.: Afforestation for climate change mitigation: Potentials, risks and trade-offs, Global Change Biology, 26, 1576-1591, 2020.

[22] Entekhabi, D., Rodriguez-Iturbe, I., and Castelli, F.: Mutual interaction of soil moisture state and atmospheric processes, Journal of Hydrology, 184, 3-17, 1996.

[23] Feng, T., Wei, W., Chen, L., Rodrigo-Comino, J., Die, C., Feng, X., Ren, K., Brevik, E. C., and Yu, Y.: Assessment of the impact of different vegetation patterns on soil erosion processes on semiarid loess slopes, Earth Surface Processes and Landforms, 43, 1860-1870, 2018.

[24] Fensholt, R., Langanke, T., Rasmussen, K., Reenberg, A., Prince, S. D., Tucker, C., Scholes, R. J., Le, Q. B., Bondeau, A., and Eastman, R.: Greenness in semi-arid areas across the globe 1981–2007—an Earth Observing Satellite based analysis of trends and drivers, Remote sensing of environment, 121, 144-158, 2012.

[25] Foley, J. A., Prentice, I. C., Ramankutty, N., Levis, S., Pollard, D., Sitch, S., and Haxeltine, A.: An integrated biosphere model of land surface processes, terrestrial carbon balance, and vegetation dynamics, Global biogeochemical cycles, 10, 603-628, 1996.

[26] Franks, S., Beven, K. J., Quinn, P., and Wright, I.: On the sensitivity of soil-vegetation-atmosphere transfer (SVAT) schemes: equifinality and the problem of robust calibration, Agricultural and Forest Meteorology, 86, 63-75, 1997.

[27] Gao, H., and Huang, Y.: Impacts of the Three-North shelter forest program on the main soil nutrients in Northern Shaanxi China: A meta-analysis, Forest Ecology and Management, 458, 117808, 2020.

[28] Gong, P., Li, X., and Zhang, W.: 40-Year (1978–2017) human settlement changes in China reflected by impervious surfaces from satellite remote sensing, Science Bulletin, 64, 756-763, 2019.

[29] Granier, A.: Evaluation of transpiration in a Douglas-fir stand by means of sap flow measurements, Tree physiology, 3, 309-320, 1987.

[30] Guo, M.-s., Ding, G.-d., Gao, G.-l., Zhang, Y., Cao, H.-y., and Ren, Y.: Community composition of ectomycorrhizal fungi associated with Pinus sylvestris var. mongolica plantations of various ages in the Horqin Sandy Land, Ecological Indicators, 110, 105860, 2020.

[31] Han, Z., Huang, S., Huang, Q., Bai, Q., Leng, G., Wang, H., Zhao, J., Wei, X., and Zheng, X.: Effects of vegetation restoration on groundwater drought in the Loess Plateau, China, Journal of Hydrology, 591, 125566, 2020.

[32] Harmon, M. E.: Carbon sequestration in forests: addressing the scale question, Journal of Forestry, 99, 24-29, 2001.

[33] Helvey, J., and Patric, J.: Canopy and litter interception of rainfall by hardwoods of eastern United States, Water Resources Research, 1, 193-206, 1965.

[34] Jia, X., Zhu, Y., and Luo, Y.: Soil moisture decline due to afforestation across the Loess Plateau, China, Journal of Hydrology, 546, 113-122, 2017.

[35] Krause, A., Pugh, T. A., Bayer, A. D., Li, W., Leung, F., Bondeau, A., Doelman, J. C., Humpenöder, F., Anthoni, P., and Bodirsky, B. L.: Large uncertainty in carbon uptake potential of land-based climate-change mitigation efforts, Global change biology, 24, 3025-3038, 2018.

[36] Li, D., Wen, L., Zhang, W., Yang, L., Xiao, K., Chen, H., and Wang, K.: Afforestation effects on soil organic carbon and nitrogen pools modulated by lithology, Forest Ecology and Management, 400, 85-92, 2017.

[37] Li, Y., Piao, S., Li, L. Z., Chen, A., Wang, X., Ciais, P., Huang, L., Lian, X., Peng, S., and Zeng, Z.: Divergent hydrological response to large-scale afforestation and vegetation greening in China, Science Advances, 4, eaar4182, 2018.

[38] Li, Z., and Pan, J.: Spatiotemporal changes in vegetation net primary productivity in the arid region of Northwest China, 2001 to 2012, Frontiers of earth science, 12, 108-124, 2018.

[39] Lu, C., Zhao, T., Shi, X., and Cao, S.: Ecological restoration by afforestation may increase groundwater depth and create potentially large ecological and water opportunity costs in arid and semiarid China, Journal of Cleaner Production, 176, 1213-1222, 2018.

705 [40] Manzoni, S., Vico, G., Porporato, A., and Katul, G.: Biological constraints on water transport in the

soil–plant–atmosphere system, Advances in Water Resources, 51, 292-304, 2013.

[41] Marin, C. T., Bouten, W., and Sevink, J.: Gross rainfall and its partitioning into throughfall,

stemflow and evaporation of intercepted water in four forest ecosystems in western Amazonia,

Journal of hydrology, 237, 40-57, 2000.

710 [42] Maxwell, R. M., Chow, F. K., and Kollet, S. J.: The groundwater–land-surface–atmosphere

connection: Soil moisture effects on the atmospheric boundary layer in fully-coupled simulations,

Advances in Water Resources, 30, 2447-2466, 2007.

[43] Meng, S., Xie, X., Zhu, B., and Wang, Y.: The relative contribution of vegetation greening to the

hydrological cycle in the Three-North region of China: A modelling analysis, Journal of

715 Hydrology, 591, 125689, 2020.

[44] Ortiz, A. M. D., Outhwaite, C. L., Dalin, C., and Newbold, T.: A review of the interactions between

biodiversity, agriculture, climate change, and international trade: research and policy priorities,

One Earth, 4, 88-101, 2021.

[45] Panwar, A., Renner, M., and Kleidon, A.: Imprints of evaporative conditions and vegetation type in

720 diurnal temperature variations, Hydrology and Earth System Sciences, 24, 4923-4942, 2020.

[46] Piao, S., Wang, X., Park, T., Chen, C., Lian, X., He, Y., Bjerke, J. W., Chen, A., Ciais, P., and

Tømmervik, H.: Characteristics, drivers and feedbacks of global greening, Nature Reviews Earth

& Environment, 1, 14-27, 2020.

[47] Shao, R., Zhang, B., Su, T., Long, B., Cheng, L., Xue, Y., and Yang, W.: Estimating the increase in

725 regional evaporative water consumption as a result of vegetation restoration over the Loess

Plateau, China, Journal of Geophysical Research: Atmospheres, 124, 11783-11802, 2019.

[48] Shi, Y., Jin, N., Ma, X., Wu, B., He, Q., Yue, C., and Yu, Q.: Attribution of climate and human

activities to vegetation change in China using machine learning techniques, Agricultural and

Forest Meteorology, 294, 108146, 2020.

730 [49] Su, B., and Shangguan, Z.: Decline in soil moisture due to vegetation restoration on the Loess Plateau of China, Land Degradation & Development, 30, 290-299, 2019.

[50] Wang, K., Ma, Z., Zhang, X., Ma, J., Zhang, L., and Zheng, J.: Effects of vegetation on the distribution of soil water in gully edges in a semi-arid region, Catena, 195, 104719, 2020a.

[51] Wang, X., Xiao, X., Zou, Z., Chen, B., Ma, J., Dong, J., Doughty, R. B., Zhong, Q., Qin, Y., and
735 Dai, S.: Tracking annual changes of coastal tidal flats in China during 1986–2016 through analyses of Landsat images with Google Earth Engine, Remote Sensing of Environment, 238, 110987, 2020b.

[52] Wei, J., and Dirmeyer, P. A.: Sensitivity of land precipitation to surface evapotranspiration: A nonlocal perspective based on water vapor transport, Geophysical Research Letters, 46, 12588-
740 12597, 2019.

[53] Wei, W., Feng, X., Yang, L., Chen, L., Feng, T., and Chen, D.: The effects of terracing and vegetation on soil moisture retention in a dry hilly catchment in China, Science of the Total Environment, 647, 1323-1332, 2019.

[54] Wu, X., Wei, Y., Fu, B., Wang, S., Zhao, Y., and Moran, E. F.: Evolution and effects of the social-
745 ecological system over a millennium in China's Loess Plateau, Science advances, 6, eabc0276, 2020.

[55] Xiao, W., Zhang, W., Ye, Y., Lv, X., and Yang, W.: Is underground coal mining causing land degradation and significantly damaging ecosystems in semi-arid areas? A study from an Ecological Capital perspective, Land Degradation & Development, 31, 1969-1989, 2020.

750 [56] Yan, F., Wu, B., and Wang, Y.: Estimating spatiotemporal patterns of aboveground biomass using Landsat TM and MODIS images in the Mu Us Sandy Land, China, Agricultural and forest meteorology, 200, 119-128, 2015.

[57] Yang, L., Zhang, H., and Chen, L.: Identification on threshold and efficiency of rainfall replenishment to soil water in semi-arid loess hilly areas, Science China Earth Sciences, 61, 292-
755 301, 2018.

[58] Yu, X., Huang, Y., Li, E., Li, X., and Guo, W.: Effects of rainfall and vegetation to soil water input and output processes in the Mu Us Sandy Land, northwest China, Catena, 161, 96-103, 2018.

[59] Yu, Y., Pi, Y., Yu, X., Ta, Z., Sun, L., Disse, M., Zeng, F., Li, Y., Chen, X., and Yu, R.: Climate change, water resources and sustainable development in the arid and semi-arid lands of Central Asia in the past 30 years, Journal of Arid Land, 11, 1-14, 2019.

[60] Zeng, Y., Yang, X., Fang, N., and Shi, Z.: Large-scale afforestation significantly increases permanent surface water in China's vegetation restoration regions, Agricultural and Forest Meteorology, 290, 108001, 2020.

[61] Zhang, J., Ding, Z., and Luo, M.: Risk analysis of water scarcity in artificial woodlands of semi-arid and arid China, Land Use Policy, 63, 324-330, 2017.

[62] Zhang, S., Yang, D., Yang, Y., Piao, S., Yang, H., Lei, H., and Fu, B.: Excessive afforestation and soil drying on China's Loess Plateau, Journal of Geophysical Research: Biogeosciences, 123, 923-935, 2018.

[63] Zhang, Y.-f., Wang, X.-p., Hu, R., Pan, Y.-x., and Paradeloc, M.: Rainfall partitioning into throughfall, stemflow and interception loss by two xerophytic shrubs within a rain-fed re-vegetated desert ecosystem, northwestern China, Journal of Hydrology, 527, 1084-1095, 2015.

[64] Zhao, M., Geruo, A., Zhang, J., Velicogna, I., Liang, C., and Li, Z.: Ecological restoration impact on total terrestrial water storage, Nature Sustainability, 1-7, 2020.

[65] Zhao, Y., Wang, Y., Wang, L., Zhang, X., Yu, Y., Jin, Z., Lin, H., Chen, Y., Zhou, W., and An, Z.: Exploring the role of land restoration in the spatial patterns of deep soil water at watershed scales, Catena, 172, 387-396, 2019.

[66] Zheng, J., Fan, J., Zhang, F., Yan, S., Guo, J., Chen, D., and Li, Z.: Mulching mode and planting density affect canopy interception loss of rainfall and water use efficiency of dryland maize on the Loess Plateau of China, Journal of Arid Land, 10, 794-808, 2018.

780   [67] Zhou, M., Wang, X., Ren, X., and Zhu, B.: Afforestation and deforestation enhanced soil CH4

uptake in a subtropical agricultural landscape: Evidence from multi-year and multi-site field

experiments, Science of The Total Environment, 662, 313-323, 2019.